# Journal Pre-proof


Thermodynamic and Kinetics Investigation of Elemental Evaporation from Molten Al7Si4Cu Alloy

Aleksandar M. Mitrašinović (Conceptualization) (Methodology) (Validation) (Formal analysis) (Investigation) (Writing - original draft) (Writing - review and editing) (Visualization) (Project administration), Zoran Odanović (Writing - review and editing) (Supervision) (Project administration) (Funding acquisition)

PII: S0040-6031(20)30731-0

DOI: https://doi.org/10.1016/j.tca.2020.178816

Reference: TCA 178816

To appear in: *Thermochimica Acta*

Received Date: 26 August 2020

Revised Date: 17 November 2020

Accepted Date: 18 November 2020

Please cite this article as: Mitrašinović AM, Zoran O, Thermodynamic and Kinetics Investigation of Elemental Evaporation from Molten Al7Si4Cu Alloy, *Thermochimica Acta* (2020), doi: https://doi.org/10.1016/j.tca.2020.178816

# Thermodynamic and Kinetics Investigation of Elemental Evaporation from Molten Al7Si4Cu Alloy

Authors: Aleksandar M. Mitrašinović[a,b,*] and Zoran Odanović[c]

[a)] Department of Materials Science and Engineering, 184 College Street, M5S 3E4, University of Toronto, Toronto, Canada

[b)] Institute of Technical Sciences of the Serbian Academy of Sciences and Arts, 35/IV Knez Mihailova, 11000 Belgrade, Serbia

[c)] Institute for testing of materials - IMS Institute, Bulevar Vojvode Misica 43, Belgrade, Serbia

[*)] Corresponding author: Ph.D. Aleksandar M. Mitrašinović; E-mail address: alex.mitrasinovic@utoronto.ca

## Highlights

- The method for removal of unwanted components from the Al alloys is presented.
- The key thermodynamic and kinetic parameters for elemental evaporation are given.
- The elemental evaporation susceptibilities are described and calculated.
- Major contaminants have the highest evaporation rates.
- Losses of the major alloying elements are minimal.

**Abstract**

Treatment of liquid aluminum alloys in low vacuum conditions is often applied for parts production in the automotive and aerospace industry because of its effectiveness in removing dissolved gases. Because of the low vapour pressure of aluminum, concentrations of the most unwanted elements can be significantly reduced at lower pressures. Presented work analyzing kinetics parameters for elemental evaporation from liquid Al7Si4Cu alloy. The pressure inside mullite refractory material was below 2.1 kPa for melt temperatures between 760 and 910 $^{o}$C. The alloy's chemical composition was characterized by the Inductively Coupled Plasma Mass Spectrometry method. Lead, Zinc, and Mercury were reduced at the highest rate while the lowest evaporation occurred for key alloying elements such as Silicon and Copper. Higher evaporation rates were achieved at higher temperatures. The evaporation ratios, volatility coefficients, reaction rate constants, mass transfer coefficients, and elemental evaporation susceptibility on temperature increase were deduced for 16 elements. The obtained results confirmed that keeping molten aluminum alloys in low vacuum conditions for one hour is an efficient method in removing unwanted elements with great potential for further improvement in industrial conditions.

Keywords: Evaporation; Kinetics; Vacuum; Impurity; Reaction rate

## 1. Introduction

Each year the demand for high quality parts in the automotive and aerospace industry grows significantly [1]. Increased environmental concerns are moving parts producers toward using purer mixtures because of their higher ductility and strength that increase durability, parts lifespan, and reusability [2]. The major feedstock for aluminum alloys is recycled materials that contain a large number and high concentration of unwanted elements. Unwanted elements contribute to the significant deterioration in the mechanical properties [3]. The value of aluminum alloys can be increased by adopting a technique capable of reducing the concentration of impurity elements in recycled alloy to low ppm levels while allowing for high capacity processes in existing facilities without the demand for large capital costs.

For a long time, high temperature refining principles at low vacuum conditions are employed for degassing and decarburization in secondary steelmaking. Bauer et al. [4] presented thermodynamic parameters that lead to the vacuum refining processes where unwanted carbon is removed with minimal losses of chromium and other alloying elements. Capurro et al. [5] reported about a 60% reduction in inclusion density in liquid steel after vacuum degassing. Mitrašinović et al. [6] showed a similar effect on silicon after treatment at temperatures around 1600 $^{o}$C and pressure below 5 kPa where inclusions settled at the tiny layer at the top edge of crucible whiles the trace elements concentrations in bulk were reduced several times. Jia et al. [7] successfully separated tin and lead originated from soldering materials by using a simple vacuum distillation method. The vacuum induction

melting method is increasingly using for the synthesis of the high entropy alloys [8]. In the aluminum industry, keeping liquid alloy in a low vacuum environment is used for the removal of dissolved hydrogen and other gases. However, low pressure treatment reduces the amounts of all elements present in the liquid alloy. Kumar and Sundarraj [9] suggested a combination of the foaming technique and low pressure for porosity assessment in Al-Si eutectic alloys and also reported changes in the chemical composition of some non-alloying elements. Subsequently, Mitrašinović and D'Souza [10] confirmed a noticeable change in chemical composition in Al7Si4Cu alloy naturally cooled from 760 $^{o}$C at 2.1 kPa although they induced low pressure only during the solidification period and at relatively low temperatures. Hence, the concentration decrease of various unwanted constituents from the aluminum alloy kept in low vacuum conditions seems to be a viable assumption.

Present work has been carried out to determine evaporation parameters for major contaminants and alloying elements in the molten secondary aluminum alloy kept in low vacuum conditions. Experiments were conducted at temperatures between 760 to 910 $^{o}$C and the elemental evaporation ratios, volatility coefficients, reaction rate constants, and transfer coefficients were deduced. Elemental evaporation susceptibility on temperature increase was quantified from the calculated kinetics parameters.

## 2. Thermodynamic Considerations

The volatility criteria and the theoretical considerations related to the evaporation reactions of substances in a low pressure environment are based on the Hertz–Knudsen equation where the maximum molar flux of evaporation of the particular element ($\acute{\eta}_{E,}\left[\frac{mol_E}{m^2\,s}\right]$) is in a direct correlation with the temperature at the interface ($T$), molar mass ($M$), the standard vapour pressure of a particular element ($p^o$), and pressure above the liquid bath ($p$).

$$\acute{\eta}_E = \frac{p^o - p}{\sqrt{2\pi MRT}} \qquad (1)$$

However, in the late 1990s, Fang and Ward [11] recognized temperature discrepancies at melt surface and emphasized that the experimental reports focused on the determination of evaporation rate constant differentiate from the theoretical predictions. Buliński et al. [12] extensively discussed the mathematical model of the complex evaporation process within a vacuum induction furnace. They found an overall agreement between experimental results and theoretical estimates. Hołyst et al. [13] used molecular dynamics simulations on a wide range of thermodynamic sets and reported up to 3.6 times higher evaporating fluxes than that Hertz–Knudsen equation would give. Likewise, large numbers of semi-empirical equations were suggested with the necessity to incorporate many factors that influence the evaporation process(es).

**Figure 1** shows changes in elements vapour pressure with temperature and pressure where elements above the aluminum vapour pressure curve will stay in liquid alloy while elements below the aluminum vapour pressure curve should readily evaporate. Because of the relatively low vapour pressure of aluminum, most of the unwanted elements can be significantly reduced by the low pressure treatment. Assessing only thermodynamic parameters provides the viability of a particular process. However, to quantify the efficiency of refining processes, kinetics parameters must be calculated.

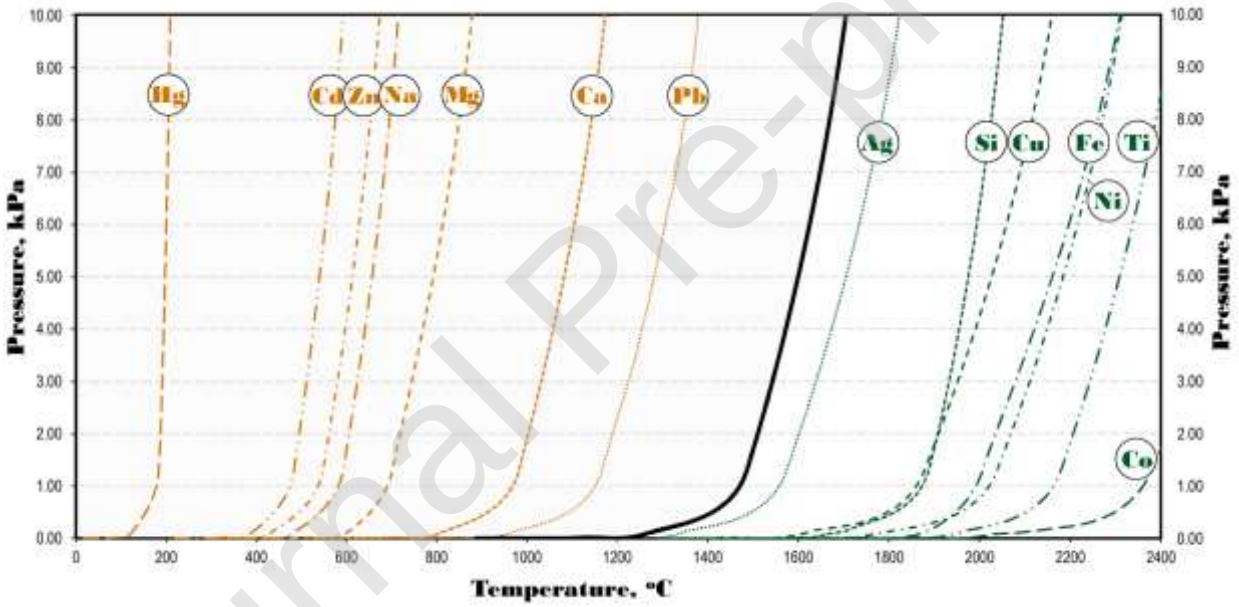


**Fig. 1** The changes in vapour pressure curves with the temperature of the most common impurities and alloying elements. Elements above the Aluminum vapour pressure curve will stay in a liquid alloy, while elements below the aluminum vapour pressure curve should readily evaporate from liquid aluminum. Diagram data got from the HSC Chemistry 5 Thermochemical Calculation Software.

## 3. Experimental Setup for Kinetics Investigation

A refractory cylinder was positioned into the one-end-closed ceramic tube (**Figure 2**). 200 g of the aluminum alloy chunks were filled at the bottom of the mullite crucible and placed at the top of the refractory cylinder. Then, the upper refractory cylinder was rested at the top of the crucible. A brass cap encapsulated the top of the ceramic tube where airtight sealing was achieved with high temperature resistant O-rings. The molybdenum-disilicide element provided rapid heating. The B-type thermocouple was inserted through furnace insulation and located at the edge of the ceramic tube. The whole furnace was wrapped in glasswool blankets for better thermal insulation. Before melting, a 6N high purity Argon gas was flashed through the copper getter chamber to remove traces of humidity and further introduced to the interior of the mullite tube to purge oxygen and other potentially chemically active gases. The lowest achieved pressure inside mullite crucible before melting was below 1.3 kPa while during experiments at high temperatures pressure was between 1.7 and 2.1 kPa. Aluminum alloy was kept for one hour at the selected temperature. Because of the high heating rate (32 K $min^{-1}$), the heating cycle did not significantly influence elemental evaporation.

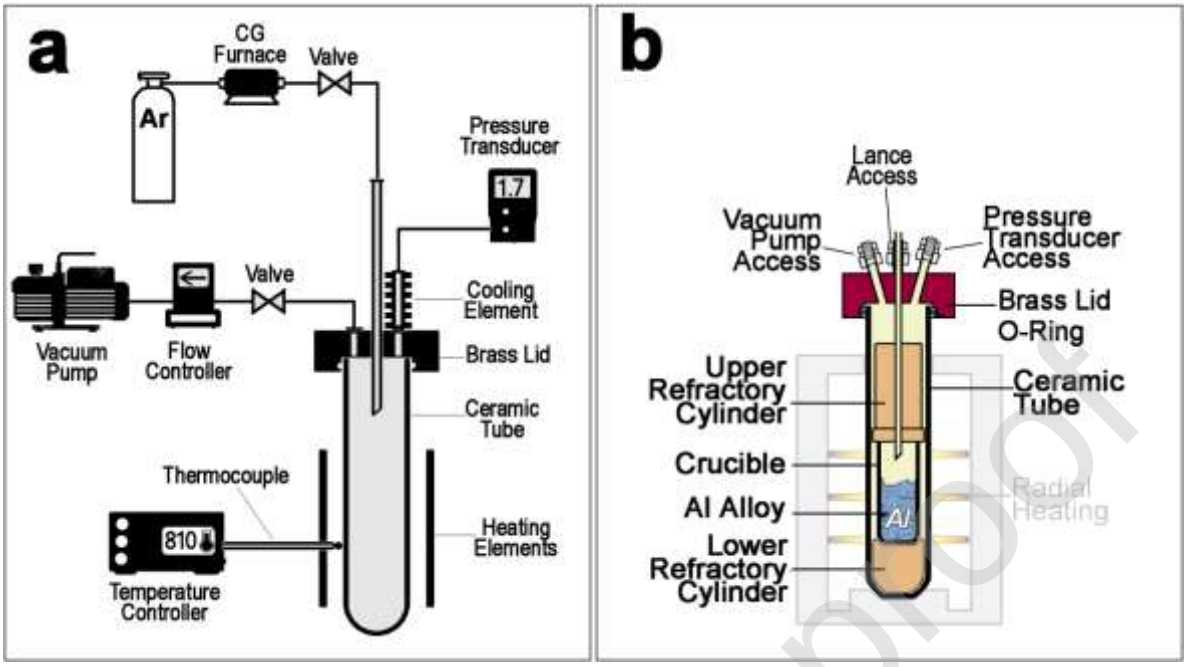


**Fig. 2** The schematics of the equipment used for low pressure tests (a) and the cross-section of the reaction tube interior designed for assessment of kinetics parameters during the elemental evaporation from the liquid alloys in a low pressure environment (b).

## 4. Selection of Vessels for Holding Aluminum Alloys in Low Vacuum

Due to the exceptionally high chemical activity of aluminum, most of the refractory materials are not suitable as containers for keeping molten aluminum in a vacuum [14, 15]. In a vacuum, the diffusion of reactive impurities instigates a chemical reaction at the solid-liquid-vapor intersection point that further accelerates the dissolution of the refractory material into a liquid bath [16]. Li et al. [17] focused on MgO refractory material containing liquid steel and found a similar mechanism causing higher concentrations of

MgO in slags for steels with higher concentrations of aluminum and carbon. Ivanov et al. [18] showed an advantage of using graphite based refractory materials during induction heating where the prime concern is the operating environment because of intensive mass flow. The refractory vessels used at high temperatures and low pressure must satisfy harsher requirements than refractory used in conventional processes, such as high thermoshock resistance and structural stability, low wettability, and thermochemical susceptibility. With advances in 3D printing technologies, oxide refractory powders are becoming the most suitable materials for ceramic core fabrication [19]. **Table 1** shows selected refractory materials commonly used as containers for aluminum evaporation processes. While metallic containers such as W, Mo, and Ta are found mostly in laboratory refractory oxides allow higher capacities and higher longevity required for the industrial environment.

In a previous investigation conducted by Mitrašinović et al. [6] related to the removal of unwanted elements from the liquid bath of silicon, a mullite refractory showed the best tradeoff between scalability required for industrial applications and structural imperviousness on high temperature. Moreover, oxygen solubility in aluminum at a melting point is $3x10^{-8}$ at% [20] and doesn't change significantly in the temperature range from 660 to 900 $^{o}$C. In practical application, these amounts are small to harm the properties of cast aluminum [21].

Table1 Thermo-physical properties of aluminum and the most common refractory materials used as containers in evaporation applications.

| Material | Density @20°C, g $cm^{-3}$ | Melting point, °C | Boiling point, °C | Tensile modulus, GPa | Thermal conductivity, W $m^{-1}$ $K^{-1}$ | Coeff. of linear thermal expansion, µm $m^{-1}$ $K^{-1}$ | Latent heat of melting, kJ $kg^{-1}$ |
|---|---|---|---|---|---|---|---|
| Al | 2.7 | 660 | 2519 | 69 | 235 | 23.1 | 396 |
| Mo | 10.28 | 2623 | 4639 | 329 | 139 | 4.8 | 375 |
| Ta | 16.65 | 3017 | 5458 | 186 | 57 | 6.3 | 199 |
| W | 19.3 | 3422 | 5555 | 411 | 170 | 4.5 | 285 |
| MgO | 3.60 | 3080 | 3600 | 270-330 | 45-60 | 9-12 | 1670-1880 |
| Alumina | 3.5-3.98 | 2004-2096 | 2977 | 215-413 | 30 | 8.1 | 620-1360 |
| Graphite | 1.61-2.43 | nf | 3600 | 4.1-27.6 | 25-470 | 0.6-8.2 | 1600-1810 |
| Mullite | 2.7-3.16 | 1750-1840 | nf | 91-220 | 1.9-6.0 | 5.3 | 314-1200 |
| Silica | 2.17-2.65 | 1710 | 2950 | 66.3-74.8 | 1.4-12 | 0.55-0.75 | 159.8 |

Data were taken from the WCSoftware database. However, due to large discrepancies in thermo-physical data for refractory materials at high temperatures data in this table should be considered as informative rather than exact values.

nf – not found

## 5. Gravimetric Analysis

In the current research, the boundary between Al7Si4Cu alloy specimen and mullite crucible was at least ten microns thick because of significant shrinkage of the alloy during the cooling period. The dissolution of aluminum or silicon from refractory material into the specimen or elemental dissolution from alloy into the refractory material is not observed.

The change in specimens weights for four holding temperatures are given in **Table 2**. Overall mass loss due to evaporation in all instances was below one percent where the only specimen kept at 910 $^{o}$C had considerably higher mass loss compared to specimens kept at temperatures below 860 $^{o}$C. Though evaporated material is mostly condensed at the upper refractory cylinder resting at the top of the mullite crucible and that material can be used as high-purity vapour-deposited directionally solidified aluminum.

Table 2 Weight change in 200g specimens kept for one hour in low-vacuum conditions.

| Melt temperature, $^{o}$C | Pressure, kPa | Sample mass, g | Percent loss, % |
|---|---|---|---|
| 760 | 1.7 | 199.5 | 0.25 |
| 810 | 1.7 | 199.3 | 0.35 |
| 860 | 1.8 | 199.0 | 0.50 |
| 910 | 2.1 | 198.1 | 0.95 |

## 6. Chemical Analysis

Four melt temperatures were investigated: 760, 810, 860, and 910 $^{o}$C. **Table 3** shows the chemical composition of the Al7Si4Cu alloy after one hour treatment at given temperatures. All elements evaporated at a higher rate than aluminum, where the lowest concentrations of all elements were at 910 $^{o}$C melt temperature. While the highest losses were recorded for the most detrimental elements in aluminum alloys such as Cd, Hg, and Pb the lowest evaporation ratio is measured for Si and Cu that are major alloying elements. Among alloying elements, only Mn had a relatively high concentration-decrease ratio.

Elements such as As, Ba, Bi, K, La, and Sc weren't detected in initial specimens by the Inductively Coupled Plasma Mass Spectrometry method and therefore couldn't be analyzed. Significant evaporation at 760 $^{o}$C was registered only for Cd, Hg, Pb, Sn, and Zn whereas at temperatures above 810 $^{o}$C evaporation rate increases significantly. While most of the obtained results are in correlation with theoretical expectations, the evaporation of elements such as Mo and Ti is difficult to explain. Some elements form oxides and separate into a tiny slag layer formed at the top of the specimen, while other form oxides that easily volatilize. Shaffer et al. [22] reported the process by which Mo formed volatile oxides. Similarly, Morita and Miki [23] explained the removal of Boron from the liquid Silicon by the formation of volatile hydrides. Zhang at al. [24] reported significant evaporation of Ti during the distillation of rare elements while Cu showed the opposite tendency. Recently, Arachchige et al. [25] detected the presence of $TiO_2$ in an oxygen pure environment. If highly volatile $Ti_2O_3$ is formed then the removal of Ti from aluminum melt could be explained.

Table 3 Change in the chemical composition ($ppm_{wt}$) in the Al7Si4Cu alloy specimens kept in low-vacuum for one hour at different temperatures.

| Element | Detection limit, $ppm_w$ | Method sensitivity, $ppm_w$ | Initial composition, $ppm_w$ | 760 °C | 810 °C | 860 °C | 910 °C |
|---|---|---|---|---|---|---|---|
| Al | - | - | Rest | Rest | Rest | Rest | Rest |
| Ag | 1 | 1 | 9 | 9 | 9 | 9 | 8 |
| Cd | 1 | 1 | 21 | 20 | 19 | 17 | 16 |
| Co | 1 | 1 | 17 | 17 | 17 | 17 | 16 |
| Cr | 1 | 1 | 230 | 230 | 220 | 220 | 210 |
| Cu | 100 | 100 | 3500 | 3500 | 3500 | 3400 | 3400 |
| Fe | 10 | 10 | 1100 | 1100 | 1070 | 1060 | 1050 |
| Hg | 5 | 5 | 30 | 25 | 20 | 10 | 5 |
| Mg | 10 | 10 | 400 | 390 | 390 | 380 | 370 |
| Mn | 1 | 1 | 250 | 250 | 240 | 240 | 230 |
| Ni | 1 | 1 | 340 | 340 | 340 | 330 | 330 |
| Pb | 10 | 10 | 400 | 390 | 390 | 350 | 290 |
| Si | 100 | 100 | 7700 | 7700 | 7700 | 7700 | 7600 |
| Sn | 1 | 1 | 30 | 29 | 29 | 28 | 27 |
| Ti | 10 | 10 | 400 | 390 | 390 | 360 | 350 |
| V | 5 | 5 | 700 | 700 | 700 | 690 | 690 |
| Zn | 1 | 1 | 180 | 180 | 170 | 170 | 160 |
| $\Sigma_{Elements}$ | - | - | 15307 | 15270 | 15204 | 14981 | 14752 |

Since evaporation is the only chemical reaction that occurs in molten aluminum alloys at temperatures below 910 °C the ratios between the amounts of impurities in the alloy before and after low pressure treatment can be expressed as an Evaporation Ratio while the change

in the amount of evaporating elements can be expressed as the Evaporated Fraction. The evaporated fraction gives the process overall purifying capacity and the quantitative result for the amount of each element removed from liquid aluminum alloy. The evaporated fraction values for 16 selected elements are given in **Figure 3**. A classification between unwanted and alloying elements in aluminum alloys depends on its intended usage. For example, Bhaduri [26] classified Sn, Sc, Zr, Ti, Sr, and Sb as favorable additions introduced to increase the mechanical properties but during recycling these elements become trace/trapped impurities. An ideal situation for alloy producers would be to have an initial alloy with only major alloying elements where they can further gauge chemical composition toward different specifications.

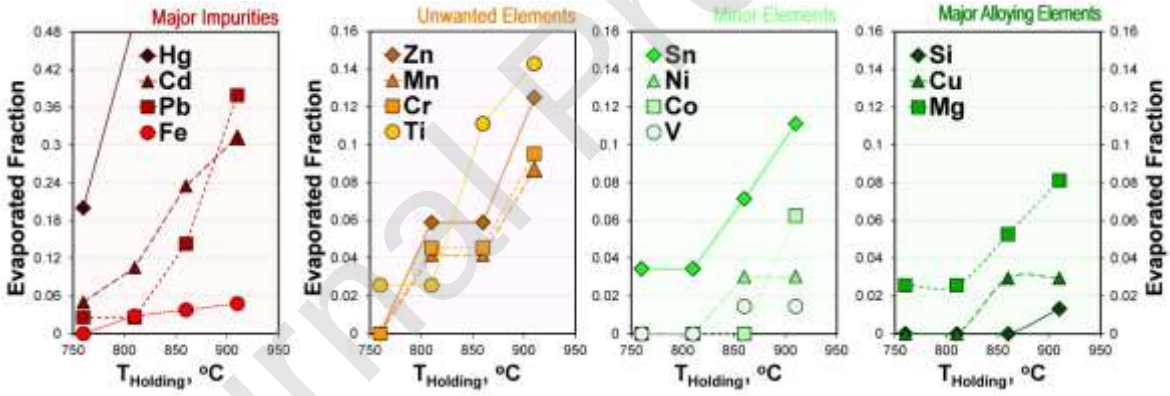


**Fig. 3** Evaporated fraction from the Al7Si4Cu alloy while kept in low-vacuum conditions for one hour.

## 7. Volatility Coefficient

The volatility coefficient ($\alpha_{Al\text{-}Xi}$) is deduced to determine the correlation between evaporation rates between aluminum and other elements. A comprehensive mathematical model for the calculation of the α in the ternary Si-Al-P system that includes a wide array of parameters affecting the evaporation process was suggested by Hoseinpur et al. [27]. In multicomponent systems where more than one volatile species are present the experimentally obtained volatility coefficient can be expressed as the ratio between the evaporation rate of solute element and each evaporating element by the following equation:

$$\alpha_{Al-Xi} = \frac{\left[\frac{c_{Al}}{c_{Al}^{Initial}}\right]}{\left[\frac{c_{Xi}}{c_{Xi}^{Initial}}\right]} \qquad (2)$$

where $C_{Xi}$ is the change in the concentration of the examined alloying element or impurity while $C_{Al}$ is the concentration of the solvent element. The numerator in Eq.2 shows a change in concentration of the solvent element concerning the overall chemical composition of the alloy. The denominator shows the change of the chemical composition of the impurity or alloying element. The volatility coefficient indicates the possibility of removing a particular element from the aluminum melt. Vacuum refining is a feasible process if both the numerator value and volatility coefficient are greater than one. If α is equal to one then the evaporation rate of solute is equal to the solvent element and therefore there is no change in overall chemical composition. If α is lower than one then negative

evaporation occurs where the solute element evaporates at a higher rate than the solvent element. At temperatures below 910 °C vacuum refining of the aluminum alloys is a feasible process since $\alpha_{Al\text{-}Al}$ is 1.0, 1.001, 1.004, and 1.007 for melt temperature of 760, 810, 860, and 910 °C, respectively. The volatility coefficients for 16 elements with respect to aluminum at temperatures between 760 and 910 °C are given in **Table 4**.

Table 4 The volatility coefficients for 16 elements with respect to aluminum ($\alpha_{Al\text{-}Xi}$).

| Element | Initial | 760 °C | 810 °C | 860 °C | 910 °C |
|---|---|---|---|---|---|
| Ag | 1.0 | 1.0004 | 1.0012 | 1.0038 | 1.1324 |
| Cd | 1.0 | 1.0505 | 1.1066 | 1.2400 | 1.3211 |
| Co | 1.0 | 1.0004 | 1.0012 | 1.0038 | 1.0695 |
| Cr | 1.0 | 1.0004 | 1.0467 | 1.0495 | 1.1024 |
| Cu | 1.0 | 1.0004 | 1.0012 | 1.0334 | 1.0362 |
| Fe | 1.0 | 1.0004 | 1.0293 | 1.0417 | 1.0545 |
| Hg | 1.0 | 1.2005 | 1.5018 | 3.0115 | 6.0393 |
| Mg | 1.0 | 1.0261 | 1.0269 | 1.0567 | 1.0882 |
| Mn | 1.0 | 1.0004 | 1.0429 | 1.0457 | 1.0941 |
| Ni | 1.0 | 1.0004 | 1.0012 | 1.0343 | 1.0371 |
| Pb | 1.0 | 1.0261 | 1.0269 | 1.1473 | 1.3883 |
| Si | 1.0 | 1.0004 | 1.0012 | 1.0038 | 1.0198 |
| Sn | 1.0 | 1.0349 | 1.0357 | 1.0756 | 1.1184 |
| Ti | 1.0 | 1.0261 | 1.0269 | 1.1154 | 1.1503 |
| V | 1.0 | 1.0004 | 1.0012 | 1.0184 | 1.0211 |
| Zn | 1.0 | 1.0004 | 1.0601 | 1.0629 | 1.1324 |

## 8. Rate Constant and Overall Mass Transfer

In chemical engineering, the determination of kinetic parameters is typically achieved by extracting a small sample for chemical analyses in a specific time frame and constructing a concentration-time curve. However, in high temperature metallurgical processes occurring inside a vacuum chamber, gaining a representative sample without disturbing the overall process is impossible. Therefore, the deduction of kinetic parameters relies only on data from the beginning and the end of a process or conducting and combining a set of tests. In this work, a set of tests with different melt temperatures is conducted, and measured elemental concentrations in solidified specimens were linked to formalize and calculate rate constants and elemental concentration related transfer coefficients. Since the elemental evaporation belongs to the first order reaction type, the change in the concentration of the examined alloying element or impurity ($X_i$) can be defined by the following general equation:

$$-\frac{d[C_{Xi}]}{dt} = k_{Xi}[C_{Xi}] \qquad (3)$$

by integrating the above equation gives

$$ln\,[C_{Xi}] = -k_{Xi}t + I_C \qquad (4)$$

where integration constant $I_c$ at the starting boundary conditions is equal to the initial concentration of a particular element (@ t=0 s, $I_C = ln\left[C_{Xi}^{Initial}\right]$) and therefore integrated form of the evaporation equation in low vacuum conditions can be written as follows:

$$ln\left[C_{Xi}^{Final}\right] = -k_{Xi}t + ln\left[C_{Xi}^{Initial}\right] \qquad (5)$$

where $C_{Xi}^{Initial}$ and $C_{Xi}^{Final}$ are the concentrations of the examined element and $t$ is treatment time. The rate constant values are typically determined from the slope of the function $-ln\left[\frac{C_{Xi}^{Final}}{C_{Xi}^{Initial}}\right]$ against time. The same approach could be used in processes where only final concentration can be measured, although a more convenient procedure would be to rearrange Equation 5 into:

$$k_{Xi} = \frac{ln\left[C_{Xi}^{Initial} - C_{Xi}^{Final}\right]}{t} \ [s^{-1}] \qquad (5a)$$

In typical liquid metal processing operations, the molten metal is contained in a refractory vessel where the only top surface is exposed to the atmosphere. Since only elements that reached the interfacial boundary between liquid alloy and vacuum can leave liquid alloy an overall elemental mass transfer ($\omega_{Xi}$) can be deduced from the experimental results by a general equation for unidirectional flow where free evaporating area and total volume of molten metal are considered:

$$\frac{dC_{Xi}}{dt} = \omega_{Xi}\frac{A}{V} \quad (6)$$

where *A* is the area describing liquid–gas boundary and *V* is the volume of the liquid metal bath. Equation 6 can be described in integral form as:

$$\int \frac{dC_{Xi}}{C_{Xi}} = -\omega_{Xi}\frac{A}{V}\int dt \quad (7)$$

that finally gives the quantified elemental mass transfer results for a particular treatment time if the interfacial area and melt volume are known:

$$ln\left(\frac{C_{Xi}^{Final}}{C_{Xi}^{Initial}}\right) = -\omega_{Xi}\frac{A}{V}t \quad (8)$$

To assess ($\omega_{Xi}$) change for different tests conducted at different temperatures, the above equation can be rearranged:

$$\omega_{Xi} = -ln\left(\frac{C_{Xi}^{Final}}{C_{Xi}^{Initial}}\right)\frac{V}{A}\frac{1}{t} \quad [\text{m s}^{-1}] \quad (8a)$$

The overall mass transfer coefficient ($\omega$) can be calculated from Equation 8a since in a particular investigation the *A/V* ratio was kept constant at 1.28 $m^{-1}$ and *t* was one hour. **Table 5** gives the overall elemental evaporation mass transfer coefficients where is apparent that $\omega$ values are significantly higher for higher melt temperatures. Further, the

effect of the melt temperature change on the overall elemental evaporation rate could be deduced from the slope of the line in $\omega$ and temperature diagram.

Table 5 The overall elemental evaporation mass transfer coefficient ($\omega$) in the Al7Si4Cu alloy specimens after one hour treatment in low-vacuum conditions.

| | $\omega$, $10^{-6}$, m $s^{-1}$ | | | |
|---|---|---|---|---|
| Element | @760 ºC | @810 ºC | @860 ºC | @910 ºC |
| Ag | 0 | 0 | 0 | 41.88 |
| Cd | 17.35 | 35.58 | 75.13 | 96.69 |
| Co | 0 | 0 | 0 | 21.55 |
| Cr | 0 | 15.8 | 15.8 | 32.34 |
| Cu | 0 | 0 | 10.31 | 10.31 |
| Fe | 0 | 9.83 | 13.17 | 16.54 |
| Hg | 64.82 | 144.16 | 390.62 | 637.07 |
| Mg | 9.01 | 9.01 | 18.24 | 27.72 |
| Mn | 0 | 14.51 | 14.51 | 29.65 |
| Ni | 0 | 0 | 10.61 | 10.61 |
| Pb | 9.01 | 9.01 | 47.48 | 114.34 |
| Si | 0 | 0 | 0 | 4.65 |
| Sn | 12.05 | 12.05 | 24.53 | 37.46 |
| Ti | 9.01 | 9.01 | 37.46 | 47.48 |
| V | 0 | 0 | 5.12 | 5.12 |
| Zn | 0 | 20.32 | 20.32 | 41.88 |

## 9. Activation Energy

The Arrhenius equation is traditionally applied in assessing the dependence of the reaction rate constants to temperature by the following equation:

$$\ln(\omega_{Xi}) = \ln(\omega_{Xi}{}^{*}) - \frac{E_{A,Xi}}{R}\frac{1}{T} \quad (9)$$

where $E_{A,Xi}$ is the activation energy for the evaporating element *Xi*. By plotting the overall elemental evaporation mass transfer coefficient (ω) obtained at various temperature ranges versus the reversed absolute temperature the activation energy ($E_{A,Xi}$) and frequency factor ($\omega_{Xi}$*) can be obtained.

**Table 6** gives values for activation energy for elements that concentration changed in the temperature range from 760 to 910 ºC. A comparison of activation energy values calculated for a wide temperature range for evaporating elements in complex alloys should be taken with the cautions. E.g., Mercury readily evaporates at lower temperatures while at higher temperatures its concentration becomes negligible and therefore difficult to calculate kinetics parameters. Lead's evaporation curve becomes very steep at temperatures above 860 ºC that indicates different values for activation energy are different at different temperature ranges. Hence, the volatility factor or elemental evaporation susceptibility assessments are more convenient methods for kinetics characteristics comparison in complex alloys treated at high temperatures and low pressures.

Table 6 The activation energy and frequency factor for evaporating elements from the Al7Si4Cu alloy at the temperature range from 760 to 910 ºC.

| | Cd | Cr | Fe | Hg | Mg | Mn | Pb | Sn | Ti | Zn |
|---|---|---|---|---|---|---|---|---|---|---|
| $\ln(\omega^*)$, $10^{-6}$ m $s^{-1}$ | -3.53 | 5.89 | -5.85 | 3.72 | -1.01 | 5.76 | 10.8 | -0.6 | 3.26 | 6.31 |
| $E_A$, kJ $mol^{-1}$ | 56.23 | 159.6 | 50.77 | 109.0 | 93.28 | 159.3 | 195.9 | 94.36 | 52.83 | 161.2 |

**10. Elemental Evaporation Susceptibility**

The evaporation rate constant (units are $s^{-1}$or m $s^{-1}$) do not contain a temperature component although it is strongly influenced by the temperature. Elemental evaporation susceptibility with respect to temperature increase can be evaluated by Equation 10:

$$\omega_{Xi} = \omega'_{Xi}\Delta T \qquad (10)$$

where $\omega'_{Xi}$ is the slope of the linear correlation between the Evaporation Mass Transfer Coefficient and the liquid melt temperature difference from the liquidus temperature of the Al7Si4Cu alloy. Since the chemical composition of the alloy doesn't change in the solid state, $\omega_{Xi}$ is considered equal to zero at liquidus temperature. **Figure 4** shows the differences in evaporation susceptibility of a particular element on the temperature increase. Similarly to the kinetics of elemental evaporation, most unwanted elements have higher

evaporation susceptibility while Si and Cu showed the lowest evaporation rate increase with an increase in liquid bath temperature.

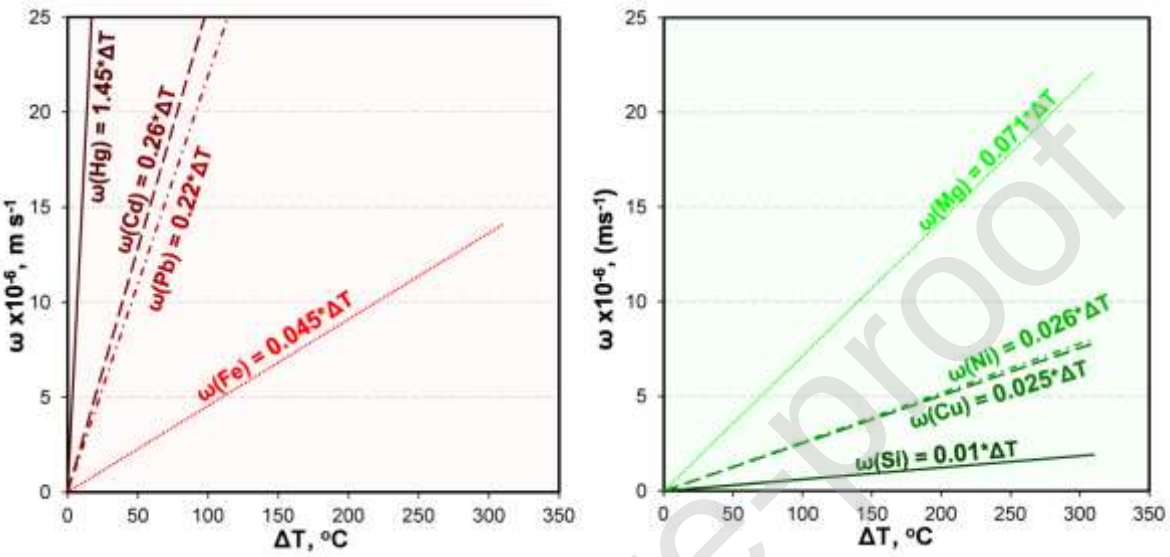


**Fig. 4** Elemental evaporation susceptibility for major impurity (a) and alloying elements (b) in Al7Si4Cu alloy during low pressure treatment.

## 11. Conclusions

An investigation on elemental evaporation from the aluminum alloys melt kept in low vacuum conditions and temperatures between 760 and 910 $^{o}$C were carried out. The results show that significant elemental evaporation in aluminum alloys occurs at temperatures above 810 $^{o}$C. The lowest losses due to evaporation were for major alloying elements such as Si and Cu while the most detrimental elements such as Hg, Pb, Cd, and Sb had the

highest evaporation ratios and elemental evaporation susceptibility concerning temperature increase. Calculated reaction rate constants for 16 elements show significantly higher values for higher melt temperatures. Obtained results allow us to conclude that the low pressure treatment traditionally used to reduce porosity and improve mechanical properties is also an effective method to reduce amounts of inclusions and impurity elements in aluminum alloys intended for the automotive and aerospace industry.

Authors Statement

Aleksandar Mitrasinovic: Conceptualization, Methodology, Validation , Formal analysis , Investigation, Writing - Original Draft, Writing - Review & Editing, Visualization, Project administration

Zoran Odanovic: Writing - Review & Editing, Supervision, Project administration, Funding acquisition

**Declaration of interests**

☒ The authors declare that they have no known competing financial interests or personal relationships that could have appeared to influence the work reported in this paper.

## Acknowledgment

This research is made possible through the unsounded kindness and support from Professor Utigard. This work was supported by the Ministry of Education, Science and Technological Development, Republic of Serbia (451-03-68/2020-14/200175).

**References**

[1] A.G. Esmeralda, A.F. Rodríguez, J. Talamantes-Silva, R. Torres, N.F. Garza-Montes-de-Oca, J.R. Benavides-Treviño, R. Colás, Thermal diffusivity of cast Al-Cu alloys. Thermochimica Acta **683** (2020) 178444

[2] D. Raabe, C.C. Tasan, E.A. Olivetti, Strategies for improving the sustainability of structural metals. Nature **575** (2019) 64

[3] J. Mathew, G. Remy, M.A. Williams, F. Tang, P. Srirangam, Effect of Fe Intermetallics on Microstructure and Properties of Al-7Si Alloys. JOM **71** (2019) 4362

[4] H. Bauer, H. Fleischer, J. Otto, Refining and decarburizing steel-degassing process in the melting practice of alloy steels. J. Vac. Sci. Technol. **7** (1970) 137

[5] C. Capurro, C. Cicutti, Steel Cleanliness Evaluation Techniques Review. Application to Different Industrial Cases. 21st IAS Steel Conference, At Rosario, Argentina, (2016) DO-10.13140/RG.2.2.21919.36005.

[6] A.M. Mitrašinović, R. D'Souza, T.A. Utigard, Impurity removal and overall rate constant during low pressure treatment of liquid silicon. Journal of Materials Processing Technology **212** (2012) 78

[7] G. Jia, B. Yang, D. Liu, Deeply removing lead from PbSn alloy with vacuum distillation. Trans. Nonferrous Met. Soc. China **23** (2013) 1822

[8] H. Wu, S. Huang, C. Zhu, J. Zhang, H. Zhu, Z. Xie, In Situ TiC/FeCrNiCu High‐Entropy Alloy Matrix Composites: Reaction Mechanism, Microstructure and Mechanical Properties. Acta Metallurgica Sinica (English Letters) **33** (2020) 1091

[9] G.S.V. Kumar, S. Sundarraj, A novel characterization technique to determine pore susceptibility of alloying elements in aluminum alloys. Metall. Mater. Trans. B **41** (2010) 495

[10] A.M. Mitrašinović, R. D'Souza, Effect of initial temperature on actual elemental evaporation rate in Al-Si-Cu mixture during free cooling in near-vacuum conditions. Vacuum **134** (2016) 99

[11] G. Fang, C.A. Ward, Temperature measured close to the interface of an evaporating liquid. Phys. Rev. **E59** (1999) 417

[12] P. Buliński, J. Smolka, G. Siwiec, L. Blacha, S. Golak, R. Przyłucki, M.Palacz, B. Melka B, Numerical examination of the evaporation process within a vacuum induction furnace with a comparison to experimental results. Applied Thermal Engineering **150** (2019) 348

[13] R. Hołyst, M. Litniewski, D. Jakubczyk, A molecular dynamics test of the Hertz-Knudsen equation for evaporating liquids. Soft Matter **11** (2015) 7201

[14] G. Kaptay, On Surface Properties of Molten Aluminum Alloys of Oxidized Surface. Materials Science Forum **77** (1991) 315

[15] A. Hoseinpur, J. Safarian, Mechanisms of graphite crucible degradation in contact with Si-Al melts at high temperatures and vacuum conditions. Vacuum **171** (2020) 108993

[16] N. Eustathopoulos, Wetting by liquid metals application in materials processing: the contribution of the grenoble group. Metals **5** (2015) 350

[17] Y. Li, W. Yang, L. Zhang, Formation Mechanism of MgO Containing Inclusions in the Molten Steel Refined in MgO Refractory Crucibles. Metals **10** (2020) 444

[18] A.N. Ivanov, V.A. Bukanin, A.E. Zenkov, Investigation of Induction Melting in Graphite Crucibles. IEEE Conference of Russian Young Researchers in Electrical and Electronic Engineering (EIConRus), (St. Petersburg and Moscow, Russia, 2020), p. 1234. doi: 10.1109/EIConRus49466.2020.9038977.

[19] H. Li, Y. Liu, Y. Liu, K. Hu, Z. Lu, J. Liang, Influence of Sintering Temperature on Microstructure and Mechanical Properties of $Al_2O_3$ Ceramic via 3D Stereolithography. Acta Metallurgica Sinica (English Letters) **33** (2020) 204

[20] S. Das, The Al-O-Ti (Aluminum-oxygen-titanium) system. Journal of Phase Equilibria **23** (2002) 525

[21] H.A. Wriedt, The AI-O (Aluminum-Oxygen) System. Bulletin of Alloy Phase Diagrams **6** (1985) 548

[22] E. Shaffer, A. Jurewicz, Jones J. Experimental studies of the volatility of V and Mn, (Lunar and Planetary Institute – NASA astrophysics data sys. LPSC XXII, 1991), P. 1221.

[23] K. Morita, T. Miki, Thermodynamics of solar-grade-silicon refining. Intermetallics **11** (2003) 1111

[24] X. Zhang, R. Miao, D. Wu, Q. Zhu, Z. Wang, D. Chen, S. Yan, Impurity distribution in distillate of terbium metal during vacuum distillation purification. Transactions of Nonferrous Metals Society of China **27** (2017) 1411

[25] H.M.M.M. Arachchige, D. Zappa, N. Poli, N. Gunawardhana, N.H. Attanayake, E. Comini, Seed-Assisted Growth of $TiO_2$ Nanowires by Thermal Oxidation for Chemical Gas Sensing. Nanomaterials **10** (2020) 935

[26] A. Bhaduri, Mechanical Properties and Working of Metals and Alloys, (Springer Nature Singapore Pte Ltd, Singapore. 2018) https://doi.org/10.1007/978-981-10-7209-3

[27] A. Hoseinpur, K. Tang, J. Safarian, Kinetic study of vacuum evaporation of elements from ternary melts; case of dilute solution of P in Si-Al melts. Separation and Purification Technology **235** (2019) 1383